

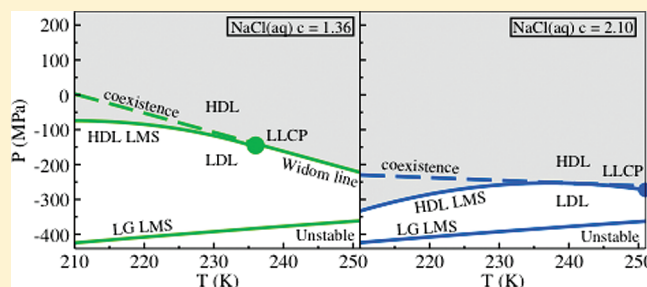
# Liquid–Liquid Coexistence in NaCl Aqueous Solutions: A Simulation Study of Concentration Effects

D. Corradini<sup>†</sup> and P. Gallo<sup>\*</sup>

Dipartimento di Fisica, Università “Roma Tre”, Via della Vasca Navale 84, I-00146 Roma, Italy

 Supporting Information

**ABSTRACT:** In this paper we investigate by means of molecular dynamics computer simulations how the hypothesized liquid–liquid critical point of water shifts in supercooled aqueous solutions of salt as a function of concentration. We study sodium chloride solutions in TIP4P water, NaCl(aq), for concentrations  $c = 1.36$  mol/kg and  $c = 2.10$  mol/kg. The liquid–liquid critical point is found up to the highest concentration investigated, and its position in the  $P$ – $T$  plane shifts to higher temperatures and lower pressures upon increasing concentration. For  $c = 2.10$  mol/kg it is also located very close to the temperature of maximum density line of the system. The results are discussed and compared with previous results for bulk TIP4P water and for  $c = 0.67$  mol/kg NaCl(aq) and with experimental findings. We observe a progressive shrinkage of the low-density liquid region when the concentration of salt increases; this suggests an eventual disappearance of the liquid–liquid coexistence upon further increase of NaCl concentration.



## I. INTRODUCTION

The polymorphic nature of supercooled water is a topic of wide interest where many open questions are still to be addressed.<sup>1–4</sup>

Two seminal papers<sup>5,6</sup> based on molecular dynamics (MD) simulations have proposed in the supercooled region of water the existence of a liquid–liquid critical point (LLCP) as the terminal point of a low-density liquid (LDL)–high-density liquid (HDL) coexistence line. This LLCP would induce long-range fluctuations able to justify the existence of the well-known thermodynamic anomalies of water such as the diverging behavior of the isothermal compressibility and of the isobaric specific heat.<sup>4,7,8</sup> Experimental evidence compatible with the existence of the LLCP have been found from the decompression-induced melting curve of ice IV giving an estimate for the position at  $P_C \sim 100$  MPa  $T_C \sim 220$  K.<sup>9</sup>

The anomalies of water can be also alternatively framed. In the singularity free scenario they are due to local density fluctuations that do not lead to singularities.<sup>10</sup> In the critical point free scenario, the LDL to HDL transition is seen as an order to disorder transition with no critical point.<sup>11</sup>

The LLCP scenario has been found in several MD simulations on water potentials (see, for example, refs 5,6, and 12–20) and on spherically symmetric potentials that mimic water behavior.<sup>15,21</sup> Upon tuning the parameters in model potentials or in theoretical models, it is possible to pass from a singularity free scenario to a LLCP scenario.<sup>22–25</sup>

Experimentally, water has never been supercooled below the temperature of homogeneous nucleation, although the possibility of reaching the glassy state by a continuous path was experimentally proven not to be forbidden.<sup>26</sup> Starting from its glassy state, the polymorphic behavior of amorphous water has been experimentally

demonstrated. Both a low-density amorphous (LDA) and an high-density amorphous (HDA) phase exist, and the coexistence line between them has been shown to be first order-like.<sup>27,28</sup> Besides, HDA appears to be thermodynamically connected to HDL, and LDA has a structure similar to LDL.<sup>3,26,29,30</sup>

Aqueous solutions can offer the possibility to experimentally reach the otherwise inaccessible region of the supercooled states and can lead therefore to an experimental determination of the LLCP.<sup>31–33</sup> In ionic solutions, the metastable region observable in experiments is extended to lower temperatures with respect to the bulk.<sup>34</sup> Detailed MD studies on the existence and the position with respect to the bulk system of the LLCP in aqueous solutions as a function of solute content are therefore of extreme interest to address experiments. The taxonomy of the LLCP in solutions of nonpolar solutes has been reported by Chatterjee and Debenedetti.<sup>31</sup> They found that upon properly tuning the strength of the dispersive interaction in their theoretical model, it was possible to move the LLCP at higher temperatures with respect to the bulk. A discrete MD study of hydrophobic solutes in Jagla water showed that the LLCP continues to exist up to at least 50% mole fraction of solutes, and it shifts progressively to lower temperatures and higher pressures.<sup>32</sup>

We have recently shown in an MD simulation on TIP4P water and  $c = 0.67$  mol/kg NaCl(aq) that in the aqueous solution the

**Special Issue:** H. Eugene Stanley Festschrift

**Received:** May 17, 2011

**Revised:** July 22, 2011

**Published:** August 18, 2011

LLCP shifts to negative pressures and higher temperatures. Its location, although at negative pressures, should be above the homogeneous nucleation line.<sup>18</sup>

In this paper we report extensive MD investigations of the phase diagram of NaCl(aq) solutions for concentration  $c = 1.36$  mol/kg  $c = 2.10$  mol/kg in the supercooled region, aimed to understand how the concentration of solutes affects the position of the LLCP.

The paper is structured as follows. The MD methods used are described in section II. In section III the results are presented and discussed. The last section, section IV, is devoted to the conclusions.

## II. METHODS

MD simulations are performed on two NaCl(aq) solutions with concentrations  $c = 1.36$  mol/kg and  $c = 2.10$  mol/kg. The results are also compared with bulk water and with  $c = 0.67$  mol/kg NaCl(aq) simulated with the same potential of a previous study.<sup>18</sup> The systems are simulated in the range of temperatures from  $T = 350$  K to  $T = 190$  K, every  $\Delta T = 5$  K, and in the range of densities from  $\rho = 1.10$  g/cm<sup>3</sup> to  $\rho = 0.87$  g/cm<sup>3</sup>, every 0.01 g/cm<sup>3</sup>. The cubic simulation box contains 256 molecules. For the  $c = 1.36$  mol/kg system  $N_{\text{wat}} = 244$  and  $N_{\text{Na}^+} = N_{\text{Cl}^-} = 6$ ; for the  $c = 2.10$  mol/kg system,  $N_{\text{wat}} = 238$  and  $N_{\text{Na}^+} = N_{\text{Cl}^-} = 9$ .

The interaction potential between particles is the sum of the electrostatic and the Lennard-Jones (LJ) potentials. The solvent molecules have been modeled using the TIP4P potential.<sup>35</sup> This potential has been shown to reproduce well the phase diagrams of supercooled<sup>6,18,36,37</sup> and crystalline<sup>38</sup> water. The ionic LJ potential interaction parameters<sup>39</sup> employed belong to a set of parameters for alkali halides tailored for use with the TIP4P potential. They were found to reproduce well the structure and free energy of hydration of ions in water. Ion–water LJ parameters were calculated using geometric mixing rules.

Long-range electrostatic interactions are treated using the Ewald summation method. The cutoff radius is set to 9.0 Å. The integration time step used is 1 fs. Temperature is controlled by a Berendsen thermostat.<sup>40</sup> We apply the following simulation protocol. For each fixed density, the initial configuration is created distributing the particles on a face-centered cubic (fcc) lattice with random orientation of water molecules. The crystal is then melted at  $T = 500$  K. From  $T = 350$  K to  $T = 190$  K the temperature is reduced stepwise every 5 K. For each temperature, an equilibration and a production run are performed. The last configuration of one temperature is used as the initial configuration for the following equilibration/production cycle. The equilibration and the production times are progressively increased with decreasing temperature. For  $c = 1.36$  mol/kg, the sum of the equilibration and production times goes from 0.15 ns for the highest temperature,  $T = 350$  K, to 30 ns for the lowest temperature,  $T = 190$  K. For  $c = 2.10$  mol/kg, it goes from 0.30 ns at  $T = 350$  K to 40 ns at  $T = 190$  K.

Total 1584 state points are collected (792 for each system). The computational time needed to perform the simulations equals more than 7 years of continuous usage of a single 2.2 GHz CPU. The simulations were performed using the parallel version of the simulations software DL\_POLY.<sup>41</sup>

The position of the LLCP is estimated from the highest point of convergence of the isochores in the  $P$ – $T$  plane<sup>12,21</sup> and from the development of a flat region in the  $P$ – $\rho$  plane. The LLCP is also the upper bound of the HDL/LDL limit of mechanical

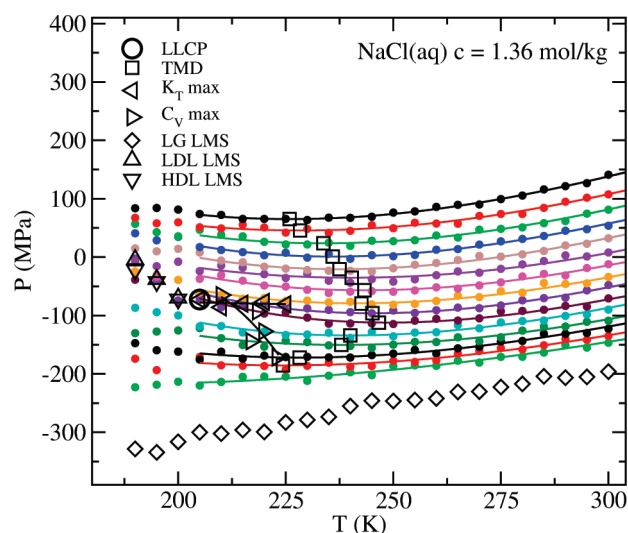


**Figure 1.** Isochores for NaCl(aq) with concentration  $c = 1.36$  mol/kg. Density spans from  $\rho = 1.10$  g/cm<sup>3</sup> (top isochore) to  $\rho = 0.96$  g/cm<sup>3</sup> (bottom isochore) with  $\Delta\rho = 0.01$  g/cm<sup>3</sup>. The state points are reported in the temperature range from  $T = 300$  K to  $T = 190$  K. Along with isochores are reported the liquid–liquid critical point (LLCP, circle) located at  $T = 205$  K and  $P = -75$  MPa, the temperature of maximum density (TMD) points (squares),  $K_T$  maxima (left pointing triangles),  $C_V$  maxima (right pointing triangles), limit of mechanical stability (LMS) points for liquid–gas (LG LMS, diamonds), low density liquid (LDL LMS, up pointing triangles) and high density liquid (HDL LMS, down pointing triangles). Solid lines joining the points are guides for the eye.

stability (LMS). The HDL/LDL LMS and liquid–gas limit of mechanical stability (LG LMS) are calculated from the points where  $(\partial P/\partial\rho)_T = 0$ . Lines of maxima of thermodynamic response functions such as the isothermal compressibility  $K_T$  and isochoric specific heat  $C_V$  also converge to the LLCP, upon merging onto the Widom line.<sup>15,36,42</sup> Maxima of  $K_T$  are calculated along isotherms and maxima of the  $C_V$  are calculated along isochores. The temperature of maximum density (TMD) points are calculated from the minima of the isochores, where the coefficient of thermal expansion  $\alpha_P$  is zero.

## III. RESULTS AND DISCUSSION

In a previous study we determined the position of the LLCP in bulk TIP4P water and in a  $c = 0.67$  mol/kg NaCl(aq) solution in TIP4P water.<sup>18</sup> The LLCP was located at  $T_c = 190$  K and  $P_c = 150$  MPa in bulk water and  $T_c = 200$  K and  $P_c = -50$  MPa in  $c = 0.67$  mol/kg NaCl(aq). Thus the position of the LLCP moves to higher temperatures and lower pressures upon adding salt to water. In this study we extend the analysis to higher concentrations of salt in order to study the direction and the magnitude of the shift of the LLCP as a function of salt concentration.

In Figure 1 we report the simulated state points for the  $c = 1.36$  mol/kg NaCl(aq) in the isochore  $P$ – $T$  plane. The isochores are reported from  $\rho = 1.10$  g/cm<sup>3</sup> to  $\rho = 0.96$  g/cm<sup>3</sup>. The  $\rho = 0.96$  g/cm<sup>3</sup> isochore is the first one not showing a minimum corresponding to the TMD. The state points are depicted for temperatures from  $T = 300$  K to  $T = 190$  K. Together with isochores, the estimated position of the LLCP, the line of  $K_T$  and  $C_V$  maxima, and the points of the TMD, LG LMS, and HDL/LDL LMS are also shown. The LLCP for  $c = 1.36$  mol/kg is located at  $T_c = 205$  K and  $P_c = -75$  MPa. Thus the same

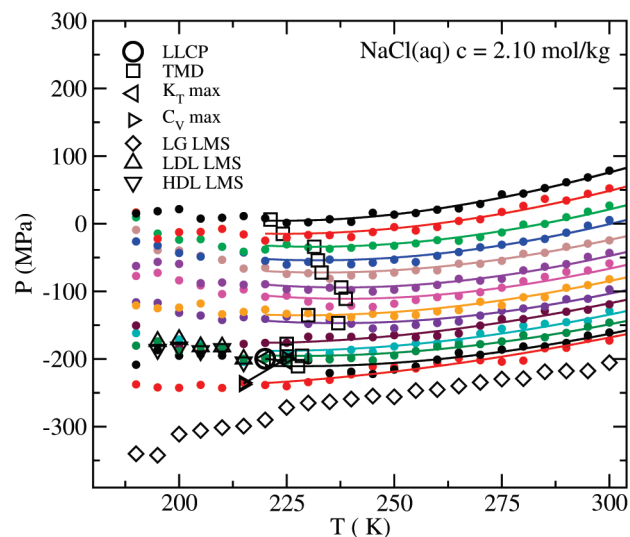


**Figure 2.** Isochores for NaCl(aq) with concentration  $c = 2.10$  mol/kg. Density spans from  $\rho = 1.10$  g/cm<sup>3</sup> (top isochore) to  $\rho = 0.97$  g/cm<sup>3</sup> (bottom isochore) with  $\Delta\rho = 0.01$  g/cm<sup>3</sup>. The state points are reported in the temperature range from  $T = 300$  K to  $T = 190$  K. Along with isochores are reported: the liquid–liquid critical point (LLCP, circle) located at  $T = 220$  K and  $P = -200$  MPa, the temperature of maximum density (TMD) points (squares),  $K_T$  maxima (left pointing triangles),  $C_V$  maxima (right pointing triangles), limit of mechanical stability (LMS) points for liquid–gas (LG LMS, diamonds), low density liquid (LDL LMS, up pointing triangles) and high density liquid (HDL LMS, down pointing triangles). Solid lines joining the points are guides for the eye.

direction of shift of the LLCP, found between bulk water and  $c = 0.67$  mol/kg, is maintained for this concentration. Namely, the LLCP moves to higher temperatures and lower pressures upon increasing concentration. The lines of  $K_T$  maxima and  $C_V$  maxima converge very close to the LLCP. Figure S1 in the Supporting Information shows the state points of  $c = 1.36$  mol/kg NaCl(aq) for all temperatures, from  $T = 350$  K to  $T = 190$  K and for densities from  $\rho = 1.10$  g/cm<sup>3</sup> to  $\rho = 0.90$  g/cm<sup>3</sup>, close to the LG LMS.

Figure 2 depicts the analogous quantities shown in Figure 1 for the  $c = 2.10$  mol/kg NaCl(aq). In this case, the isochores are reported from  $\rho = 1.10$  g/cm<sup>3</sup> to  $\rho = 0.97$  g/cm<sup>3</sup>. The  $\rho = 0.97$  g/cm<sup>3</sup> is the first isochore not displaying a minimum corresponding to the TMD. The state points are again shown for temperatures from  $T = 300$  K to  $T = 190$  K. Also for this system, the estimated position of the LLCP, the line of  $K_T$  and  $C_V$  maxima, and the points of the TMD, the LG LMS, and the HDL/LDL LMS are reported. The position of the LLCP for  $c = 2.10$  mol/kg moves further up in temperature and further down in pressure with respect to the  $c = 1.36$  mol/kg NaCl(aq), being located at  $T_c = 220$  K and  $P_c = -200$  MPa, still maintaining the trend observed starting from bulk water upon increasing the salt content. In this system, the position of LLCP is found to be very close to the TMD. The lines of  $K_T$  and  $C_V$  maxima are short and confined in a narrow region of temperature and pressure. Figure S2 in the Supporting Information shows the state points of  $c = 2.10$  mol/kg NaCl(aq) for all temperatures, from  $T = 350$  K to  $T = 190$  K and for densities from  $\rho = 1.10$  g/cm<sup>3</sup> to  $\rho = 0.94$  g/cm<sup>3</sup>, close to the LG LMS.

To better visualize how the LLCP shifts in the NaCl(aq) solutions at the different concentrations, we show in Figure 3 the positions of the LLCP in bulk TIP4P water and in  $c = 0.67, 1.36$

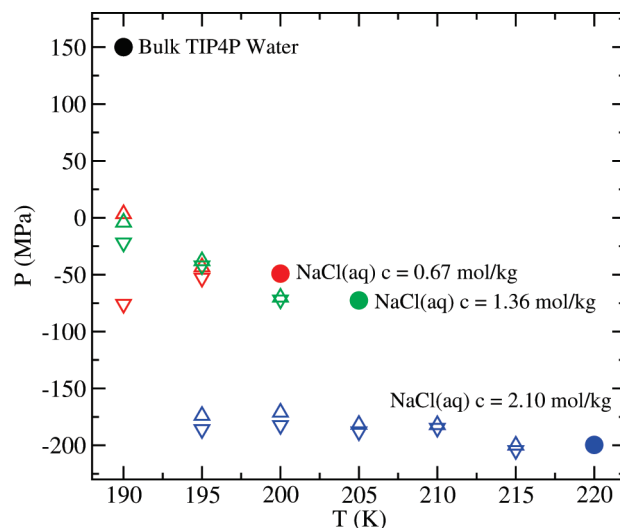


**Figure 3.** Liquid–liquid critical point (LLCP, circles) for TIP4P bulk water:  $T = 190$  K and  $P = 150$  MPa; for  $c = 0.67$  mol/kg NaCl(aq):  $T = 200$  K and  $P = -50$  MPa; for  $c = 1.36$  mol/kg NaCl(aq):  $T = 205$  K and  $P = -75$  MPa and for  $c = 2.10$  mol/kg NaCl(aq):  $T = 220$  K and  $P = -200$  MPa. For the NaCl(aq) solutions the limit of mechanical stability (LMS) points for low density liquid (LDL LMS, up pointing triangles) and high density liquid (HDL LMS, down pointing triangles) are also reported.

and 2.10 mol/kg NaCl(aq) solutions. For the solutions, the points of the HDL/LDL LMS line are also shown. The shift of the LLCP in NaCl(aq) solution is monotonic. For all the concentrations investigated, the critical temperature increases and the critical pressure decreases, upon increasing the concentration of salt. A strong reduction of the width of the region encompassed between the LDL and HDL LMS lines is also observed, when the concentration is increased. The slope of the coexistence line located in between the HDL and LDL LMS seems also to decrease upon increasing concentrations, becoming almost flat at  $c = 2.10$  mol/kg.

Our results indicate a liquid–liquid critical line for the solution originating at the LLCP. This critical line has been previously observed in theoretical models of solutions of interacting nonpolar solutes in a water-like solvent<sup>31</sup> and in simulations of solutions of hydrophobic solutes in the Jagla water-like solvent.<sup>18</sup> Moreover, it was experimentally found for NaCl(aq) that a line of liquid–gas critical points also originates from the liquid–gas critical point.<sup>43</sup> Thus the existence of a LLCP in the ionic solution for concentrations from low to moderate is an indication of the existence of the LLCP in pure water.

The position of the LLCP of the four systems is also shown in Figure 4 together with the TMD lines and the points of the LG LMS. The position of the LG LMS line is very mildly affected by the increase in the number of ions. Minor changes start to be noticeable from  $c = 1.36$  mol/kg, but the LG LMS lines lie almost at the same pressures. On the contrary, the position of the LLCP moves progressively to lower pressures when the concentration of solutes is increased. We can roughly estimate the width of the region of existence of the LDL phase measuring the distance in pressure (at the respective critical temperature) between the LLCP and the LG LMS line. If we define this difference as  $\Delta P_{LDL} = P_c - P_{LGMS}$  at  $T_c$ , then for bulk water,  $\Delta P_{LDL} \approx 510$  MPa; for  $c = 0.67$  mol/kg NaCl(aq),  $\Delta P_{LDL} \approx 250$  MPa; for  $c = 1.36$  mol/kg NaCl(aq),  $\Delta P_{LDL} \approx 225$  MPa and for

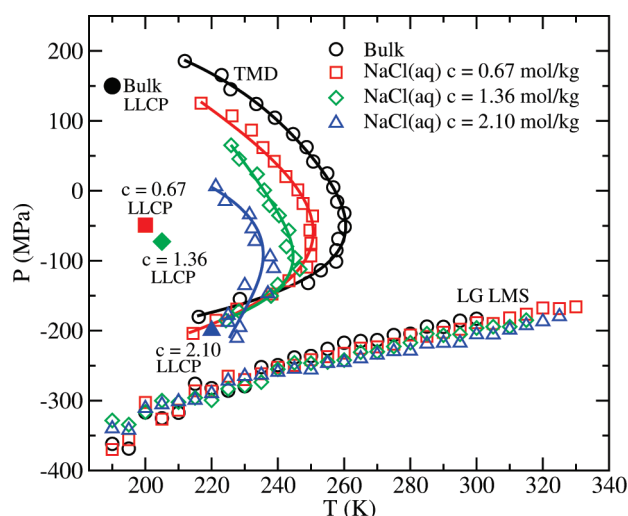


**Figure 4.** Comparison of the phase diagrams of bulk TIP4P water (black circles),  $c = 0.67$  mol/kg (red, squares),  $c = 1.36$  mol/kg (green, diamonds) and  $c = 2.10$  mol/kg (blue, triangles) NaCl(aq) solutions. The quantities shown are the liquid–liquid critical point (LLCP, filled symbols), the temperature of maximum density (TMD) points, and the liquid–gas limit of mechanical stability (LG LMS) points. The solid lines are polynomial fits to the simulated TMD points, meant as a guide for the eye.

$c = 2.10$  mol/kg NaCl(aq),  $\Delta P_{LDL} \approx 90$  MPa. Thus we see that the presence of ions progressively pushes the LDL phase toward the LG LMS line, reducing the width of its region of existence. This is to be connected with a favored solvation of ions in the HDL phase, observed in experiments on LiCl(aq)<sup>44–48</sup> and in computer simulations on solutions of model hydrophilic solutes in monoatomic mW water.<sup>49</sup> From a structural point of view, it has also been observed in computer simulations on NaCl(aq) on TIP4P water that chloride ions are able to disrupt the LDL ordered network.<sup>37</sup> Very recently Longinotti et al.<sup>50</sup> studied the thermodynamics and the dynamics of NaCl(aq) solutions in TIP4P water at ambient pressure. They also found results compatible with a stabilization of the HDL phase, induced by the ions.

Upon increasing the concentration of salt, the LLCPP also gets progressively closer to the TMD line, reducing the distance between the onset of the density anomaly and the HDL–LDL phase separation. In fact, the TMD line globally moves to lower pressures and lower temperatures when the salt content increases, and at the same time the LLCPP moves to lower pressures and to higher temperatures. To estimate the magnitude of this effect, we can define  $\Delta T_n = T_n - T_c$  as the distance between the “nose” (or turning point) of the TMD and the critical temperature. For bulk water,  $\Delta T_n \approx 70$  K; for  $c = 0.67$  mol/kg NaCl(aq),  $\Delta T_n \approx 50$  K; for  $c = 1.36$  mol/kg NaCl(aq),  $\Delta T_n \approx 40$  K; and for  $c = 2.10$  mol/kg NaCl(aq),  $\Delta T_n \approx 15$  K. Therefore we see how the LLCPP and the TMD curves become closer as the concentration increases.

We now discuss how our results can help the experimental determination of the LLCPP in aqueous systems. Many water potentials used in MD that are able to qualitatively reproduce the phase diagram of water, display a shift in temperature and pressure with respect to the behavior of experimental water. TIP4P in particular is able to reproduce very well, albeit with a shift, the complex phase diagrams of crystalline phases of water.<sup>38,51</sup>

In our previous work<sup>18</sup> we estimated that a shift in temperature of  $\Delta T = +31$  K and  $\Delta P = -73$  MPa, causes the TMD of

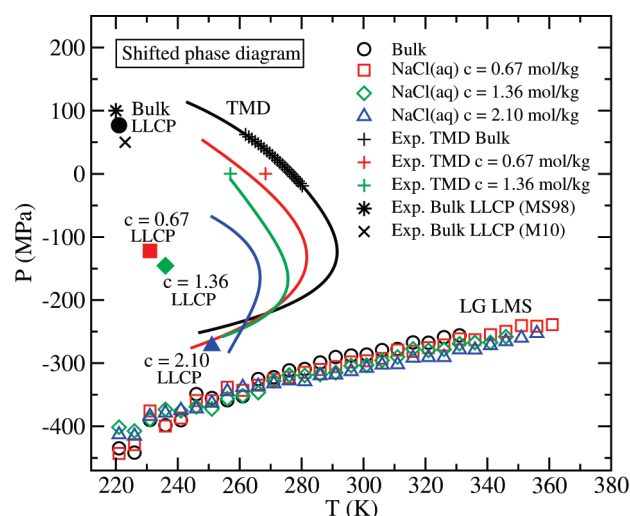


**Figure 5.** Shifted phase diagram (see text) of bulk TIP4P water (black circles),  $c = 0.67$  mol/kg (red, squares),  $c = 1.36$  mol/kg (green, diamonds) and  $c = 2.10$  mol/kg (blue, triangles) NaCl(aq) solutions. The quantities shown are the shifted liquid–liquid critical point (LLCP, filled symbols), shifted temperature of maximum density (TMD) lines from Figure 4 (solid lines), and shifted liquid–gas limit of mechanical stability (LG LMS). Experimental quantities are reported for comparison: LLCPP for bulk water as estimated by Mishima and Stanley<sup>9</sup> in 1998 (MS98) (black star), LLCPP for bulk water as estimated by Mishima<sup>52</sup> in 2010 (M10) (black cross); TMD line for bulk water (black + symbols line), fitted from available data from refs 53–56, TMD points at ambient pressure extrapolated from ref 57 for  $c = 0.67$  mol/kg (red +) and  $c = 1.36$  mol/kg (green +).

TIP4P bulk water to coincide with the experimental available data and the position of the LLCPP to be very close to the one hypothesized by Mishima and Stanley on the basis of experimental results<sup>9</sup> on the decompression-induced melting of ice IV:  $T_c \approx 220$  K and  $P_c \approx 100$  MPa. Recently, Mishima proposed a new estimate of the LLCPP of bulk water on the basis of volumetric measurements on supercooled liquid water:<sup>52</sup>  $T_c \approx 223$  K and  $P_c \approx 50$  MPa. The position of TIP4P bulk water LLCPP, after the mentioned shift,  $T_c \approx 221$  K and  $P_c \approx 77$  MPa, appears to be compatible with both experimental estimates. The shifted bulk TIP4P LLCPP and the two experimental estimates are reported in Figure 5.

In Figure 5 we also report the same quantities shown in Figure 4 after the application of the shift  $\Delta T = +31$  K and  $\Delta P = -73$  MPa, proposed for bulk water, together with the experimental values of the bulk TMD obtained from refs 53–56 and the experimental values for the TMD of  $c = 0.67$  and  $c = 1.36$  mol/kg NaCl(aq) extrapolated for these concentrations from ref 57. We apply the same shift to the solutions because we observe that the distance between the simulated TMD of NaCl(aq) and bulk water, at ambient pressure,  $\Delta T_{TMD} \approx 10$  K for  $c = 0.67$  mol/kg NaCl(aq) and  $\Delta T_{TMD} \approx 20$  K for  $c = 1.36$  mol/kg NaCl(aq) (see Figure 4) is the same found between the available experimental TMD points at ambient pressure (see Figure 5). We could not extrapolate a TMD point for  $c = 2.10$  mol/kg NaCl(aq) because, in the range of temperatures studied in ref 57, the maximum in density as a function of temperature disappears somewhere between  $c = 1.487$  mol/kg and  $c = 2.330$  mol/kg. Nonetheless, we reported shifted data for  $c = 2.10$  mol/kg also in Figure 5 for comparison with the other concentrations. We can also observe that after the

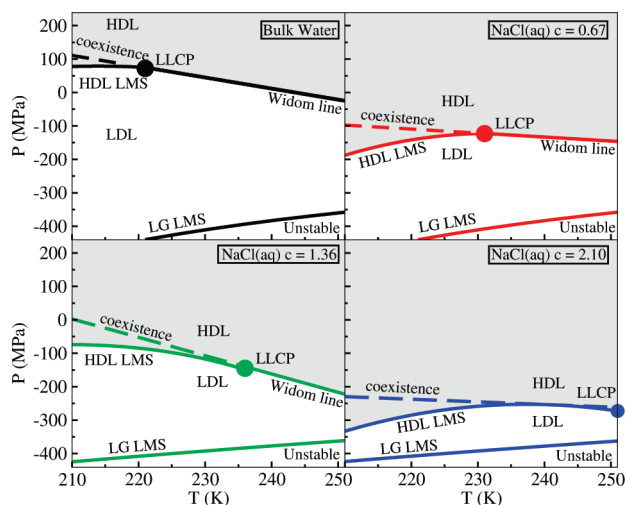


**Figure 6.** Schematic representation of the phase diagram for bulk water and for the NaCl(aq) aqueous solutions studied as they should appear in experiments.

shift the bulk TIP4P TMD line exactly superposes to available experimental values and that the shifted TMD lines for  $c = 0.67$  and  $c = 1.36$  mol/kg NaCl(aq) are found very close to the available experimental TMD points at ambient pressure.

We previously reported<sup>18</sup> that the LLCP of  $c = 0.67$  mol/kg after the application of the shift, should fall in the experimental accessible region, being located at  $T_c = 231$  K and  $P_c = -123$  MPa. In fact, the homogeneous nucleation temperature  $T_H$  shifts downward by ca. 5 K in  $c = 0.67$  mol/kg.<sup>34,58</sup> Moreover, large negative pressures have been reached in experiments on aqueous systems. In particular, for  $c = 1.00$  mol/kg NaCl(aq), rupture appears to occur below  $-140 \pm 20$  MPa.<sup>59</sup> Applying the same shift to the  $c = 1.36$  mol/kg NaCl(aq), we obtain, for the LLCP,  $T_c = 236$  K and  $P_c = -148$  MPa. Also, this value should be reachable in experiments. In fact the  $T_H$  for  $c = 1.36$  mol/kg NaCl(aq) shifts downward by ca. 10 K with respect to bulk water,<sup>34</sup>  $T_H \approx 225$  K at ambient pressure, and experimental evidence suggests that pressures as low as  $P = -150$  MPa can be reachable in aqueous solutions.<sup>59</sup>

In Figure 6 we report a schematic picture of the shifted phase diagram for bulk water and for  $c = 0.67, 1.36,$  and  $2.10$  mol/kg NaCl(aq). We focus on the  $P$ – $T$  region around the LLCP where we observe a progressive shrinkage of the LDL region upon increasing the concentration of ions in the solution. At the highest concentration investigated we observe that the LDL region has suffered a major reduction. This suggests that the LDL region and the coexistence region between HDL and LDL might completely disappear upon further increase of the salt content.

#### IV. CONCLUSIONS

In this paper we have extended our previous study on the influence of salt on water phase diagram in the supercooled region. We find that the TMD and the LLCP persist in the NaCl(aq) solutions up to the highest concentration of ions investigated,  $c = 2.10$  mol/kg. The position of the LLCP shifts monotonically to higher temperatures and lower pressures, going from bulk water to the highest concentration  $c = 2.10$  mol/kg. We also observed a progressive reduction of the region of existence of the LDL phase, upon increasing salt content. For  $c = 2.10$  mol/kg,

the region between the HDL LMS and the LG LMS line becomes very small; this suggests that the liquid–liquid coexistence will eventually disappear, upon further increase of NaCl concentration. The shift of the LLCP and the progressive reduction of the LDL region can be connected to the disruption of the ordered LDL structure induced by the ions observed when studying the structure of NaCl(aq).<sup>37</sup> Ions can in fact be more readily accommodated in the packed HDL structure. The change in HDL–LDL equilibria induced by the presence of ions in the solutions causes the LLCP to shift to higher temperatures and lower pressures, with respect to the bulk. Upon comparing our data with existing experimental data for the TMD both in the bulk and in the solutions, we predict that the LLCP should be measurable in experiments for both  $c = 0.67$  mol/kg and  $c = 1.36$  mol/kg. Although at negative pressures, difficult to reach experimentally, its location should be above the homogeneous nucleation line. Thus we have seen that the study of ionic aqueous solutions could be a very valuable tool for the study of the LLCP phenomenon in aqueous systems. In fact, the hypothesized LLCP of water, insofar still undetectable experimentally, might be measured in aqueous solutions. To this end, we plan to extend our study to solutions of other solutes, in order to see which aqueous system offers the most favorable shift of LLCP of water for its experimental determination.

#### ■ ASSOCIATED CONTENT

**S Supporting Information.** For clarity, only a portion of the state points simulated for  $c = 1.36$  mol/kg NaCl(aq) and for  $c = 2.10$  mol/kg NaCl(aq) have been reported in Figure 1 and Figure 2, respectively. The state points for all temperatures, from  $T = 350$  K to  $T = 190$  K and for densities from  $\rho = 1.10$  g/cm<sup>3</sup> to the LG LMS are shown in Figure S1 for  $c = 1.36$  mol/kg NaCl(aq) and in Figure S2 for  $c = 2.10$  mol/kg NaCl(aq). This information is available free of charge via the Internet at <http://pubs.acs.org>.

#### ■ AUTHOR INFORMATION

##### Corresponding Author

\*E-mail: gallop@fis.uniroma3.it.

##### Present Addresses

†Center for Polymer Studies and Department of Physics, Boston University, 590 Commonwealth Avenue, Boston, MA 02215, United States.

#### ■ ACKNOWLEDGMENT

We gratefully acknowledge the computational resources offered by CINECA, by CASPUR, and by the INFN RM3-GRID at Roma Tre University.

#### ■ REFERENCES

- (1) Stanley, H. E.; Kumar, P.; Xu, L.; Yan, Z.; Mazza, M. G.; Buldyrev, S. V.; Chen, S.-H.; Mallamace, F. *Physica A* **2007**, *386*, 729.
- (2) Debenedetti, P. G.; Stanley, H. E. *Phys. Today* **2003**, *56*, 40.
- (3) Mishima, O.; Stanley, H. E. *Nature (London)* **1998**, *396*, 329.
- (4) Debenedetti, P. G. *J. Phys.: Condens. Matter* **2003**, *15*, R1669.
- (5) Poole, P. H.; Sciortino, F.; Essmann, U.; Stanley, H. E. *Nature (London)* **1992**, *360*, 324.
- (6) Poole, P. H.; Sciortino, F.; Essmann, U.; Stanley, H. E. *Phys. Rev. E* **1993**, *48*, 3799.

- (7) Speedy, R. J.; Angell, C. A. *J. Chem. Phys.* **1976**, *65*, 851.
- (8) Angell, C. A. *Annu. Rev. Phys. Chem.* **1983**, *34*, 593.
- (9) Mishima, O.; Stanley, H. E. *Nature (London)* **1998**, *392*, 164.
- (10) Sastry, S.; Debenedetti, P. G.; Sciortino, F.; Stanley, H. E. *Phys. Rev. E* **1996**, *53*, 6144.
- (11) Angell, C. A. *Science* **2008**, *319*, 582.
- (12) Poole, P. H.; Saika-Voivod, I.; Sciortino, F. *J. Phys.: Condens. Matter* **2005**, *17*, L431.
- (13) Liu, Y.; Panagiotopoulos, A. Z.; Debenedetti, P. G. *J. Chem. Phys.* **2009**, *131*, 104508.
- (14) Yamada, M.; Mossa, S.; Stanley, H. E.; Sciortino, F. *Phys. Rev. Lett.* **2002**, *88*, 195701.
- (15) Xu, L.; Kumar, P.; Buldyrev, S. V.; Chen, S.-H.; Poole, P. H.; Sciortino, F.; Stanley, H. E. *Proc. Natl. Acad. Sci. U.S.A.* **2005**, *102*, 16558.
- (16) Paschek, D. *Phys. Rev. Lett.* **2005**, *94*, 217802.
- (17) Paschek, D.; Ruppert, A.; Geiger, A. *Chem. Phys. Chem.* **2008**, *9*, 2737.
- (18) Corradini, D.; Rovere, M.; Gallo, P. *J. Chem. Phys.* **2010**, *132*, 134508.
- (19) Abascal, J. L. F.; Vega, C. *J. Chem. Phys.* **2010**, *133*, 234502.
- (20) Abascal, J. L. F.; Vega, C. *J. Chem. Phys.* **2011**, *134*, 186101.
- (21) Xu, L.; Buldyrev, S. V.; Angell, C. A.; Stanley, H. E. *Phys. Rev. E* **2006**, *74*, 031108.
- (22) Roberts, C. J.; Debenedetti, P. G. *J. Chem. Phys.* **1996**, *105*, 658.
- (23) Truskett, T. M.; Debenedetti, P. G.; Sastry, S.; Torquato, S. *J. Chem. Phys.* **1999**, *111*, 2647.
- (24) Stokely, K.; Mazza, M. G.; Stanley, H. E.; Franzese, G. *Proc. Natl. Acad. Sci. U.S.A.* **2010**, *107*, 1301.
- (25) Strelakova, E. G.; Mazza, M. G.; Stanley, H. E.; Franzese, G. *Phys. Rev. Lett.* **2011**, *106*, 145701.
- (26) Speedy, R. J.; Debenedetti, P. G.; Smith, S. R.; Huang, C.; Kay, B. D. *J. Chem. Phys.* **1996**, *105*, 240.
- (27) Winkel, K.; Elsaesser, M. S.; Mayer, E.; Loerting, T. *J. Chem. Phys.* **2008**, *128*, 044510.
- (28) Kim, C. U.; Barstow, B.; Tate, M. V.; Gruner, S. M. *Proc. Natl. Acad. Sci. U.S.A.* **2009**, *106*, 4596.
- (29) Smith, R. S.; Kay, B. D. *Nature (London)* **1999**, *398*, 788.
- (30) Mallamace, F.; Broccio, M.; Corsaro, C.; Faraone, A.; Majolino, D.; Venuti, V.; Liu, L.; Mou, C.-Y.; Chen, S.-H. *Proc. Natl. Acad. Sci. U.S.A.* **2007**, *104*, 424.
- (31) Chatterjee, S.; Debenedetti, P. G. *J. Chem. Phys.* **2006**, *124*, 154503.
- (32) Corradini, D.; Buldyrev, S. V.; Gallo, P.; Stanley, H. E. *Phys. Rev. E* **2010**, *81*, 061504.
- (33) Huang, C. C.; Weiss, T. M.; Nordlund, D.; Wikfeldt, K. T.; Pettersson, L. G. M.; Nilsson, A. *J. Chem. Phys.* **2010**, *133*, 134504.
- (34) Miyata, K.; Kanno, H.; Niino, T.; Tomizawa, K. *Chem. Phys. Lett.* **2002**, *354*, 51.
- (35) Jorgensen, W. L.; Chandrasekhar, J.; Madura, J. D.; Impey, R. W.; Klein, M. L. *J. Chem. Phys.* **1983**, *79*, 926.
- (36) Sciortino, F.; Poole, P. H.; Essmann, U.; Stanley, H. E. *Phys. Rev. E* **1997**, *55*, 727.
- (37) Corradini, D.; Rovere, M.; Gallo, P. *J. Phys. Chem. B* **2011**, *115*, 1461.
- (38) Sanz, E.; Vega, C.; Abascal, J. L. F.; MacDowell, L. G. *Phys. Rev. Lett.* **2004**, *92*, 255701.
- (39) Jensen, K. P.; Jorgensen, W. L. *J. Chem. Theory Comput.* **2006**, *2*, 1499.
- (40) Berendsen, H. J. C.; Postma, J. P. M.; van Gunsteren, W. F.; DiNola, A.; Haak, J. R. *J. Chem. Phys.* **1984**, *81*, 3684.
- (41) Smith, W.; Forester, T. R.; Todorov, I. T. *The DL\_POLY\_2.0 User*; Daresbury Laboratory: Daresbury, U.K., 2006.
- (42) Franzese, G.; Stanley, H. E. *J. Phys.: Condens. Matter* **2007**, *19*, 205126.
- (43) Abdulagatov, A. I.; Stepanov, G. V.; Abdulagatov, I. M. *Therm. Eng.* **2008**, *55*, 795.
- (44) Mishima, O. *J. Chem. Phys.* **2005**, *123*, 154506.
- (45) Mishima, O. *J. Chem. Phys.* **2007**, *126*, 244507.
- (46) Souda, R. *J. Chem. Phys.* **2006**, *125*, 181103.
- (47) Suzuki, Y.; Tominaga, Y. *J. Chem. Phys.* **2011**, *134*, 244511.
- (48) Bove, L. E.; Klotz, S.; Philippe, J.; Saitta, A. M. *Phys. Rev. Lett.* **2011**, *106*, 125701.
- (49) Le, L.; Molinero, V. *J. Phys. Chem. A* **2011**, *115*, 5900.
- (50) Longinotti, M. P.; Carignano, M. A.; Szeleifer, I.; Corti, H. R. *J. Chem. Phys.* **2011**, *134*, 244510.
- (51) Vega, C.; Sanz, E.; Abascal, J. L. F. *J. Chem. Phys.* **2005**, *122*, 114507.
- (52) Mishima, O. *J. Chem. Phys.* **2010**, *133*, 144503.
- (53) Henderson, S. J.; Speedy, R. J. *J. Phys. Chem.* **1987**, *91*, 3062.
- (54) Thermophysical Properties of Fluid Systems, NIST Chemistry WebBook (2008). URL: <http://webbook.nist.gov/chemistry/fluid/>
- (55) Harrington, S.; Poole, P. H.; Sciortino, F.; Stanley, H. E. *J. Chem. Phys.* **1997**, *107*, 7443.
- (56) Hill, P. G. *J. Phys. Chem. Ref. Data* **1990**, *19*, 1233.
- (57) Archer, D. G.; Carter, R. W. *J. Phys. Chem. B* **2000**, *104*, 8563.
- (58) Kanno, H.; Speedy, R. J.; Angell, C. A. *Science* **1975**, *189*, 880.
- (59) Green, J. L.; Durben, D. J.; Wolf, G. H.; Angell, C. A. *Science* **1990**, *249*, 649.